Determining the neutrino mass ordering and oscillation parameters with KM3NeT/ORCA

Papermeeting

2021-02-04

Papermeeting

- Collecting feedback as a group
- Comments found here: https://docs.google.com/document/d/1acc2ytTAEhuxWktnow4W8Ol8oWHMDwk5hlYh9IVDesk/edit?usp=sharing
- In case we run late, feel free to add more yourself or mail it to me

Abstract

Abstract

The KM3NeT/ORCA sensitivity to atmospheric neutrino oscillations is presented according to the final detector geometry. The event reconstruction, selection and classification are described. The sensitivity to determined the NMO was evaluated and found to be 4.4σ if the true NMO is normal order (NO) and 2.3σ if inverted order (IO) after three years of data taking. The precision to measure Δm^2_{32} and θ_{23} were also estimated and found to be $85 \cdot 10^{-6}\,\mathrm{eV}^2$ and $(^{+1.9}_{-3.1})^\circ$ for NO and, $75 \cdot 10^{-6}\,\mathrm{eV}^2$ and $(^{+2.0}_{-7.0})^\circ$ for IO. Finally, a unitarity test of the leptonic mixing matrix by measuring the rate of tau neutrinos is described and one year of data taking was found to be sufficient to exclude $\overset{(-)}{\nu}_\tau$ event rate variations larger than $30\,\%$ at $3\,\sigma$ level.

determine

Introduction

- Neutrino mixing model, open questions and global fit
- ν_τ appearance and unitarity U
- NMO and mass effect
- Updates KM3NeT with respect to LOI:
  - Detector geometry
  - Improved neutrino detection efficiency
  - Improved Reconstruction

ORCA detector response

- 2.1 Detector design
- 2.2 Simulation: new ORCA trigger for faint events
- 2.3 Event topologies
- 2.4 Event reconstruction and event selection

ORCA detector response

2.4 Event reconstruction and selection

- Triggering and reco updates shifted turn on region by 20%
- Add real volume as line?

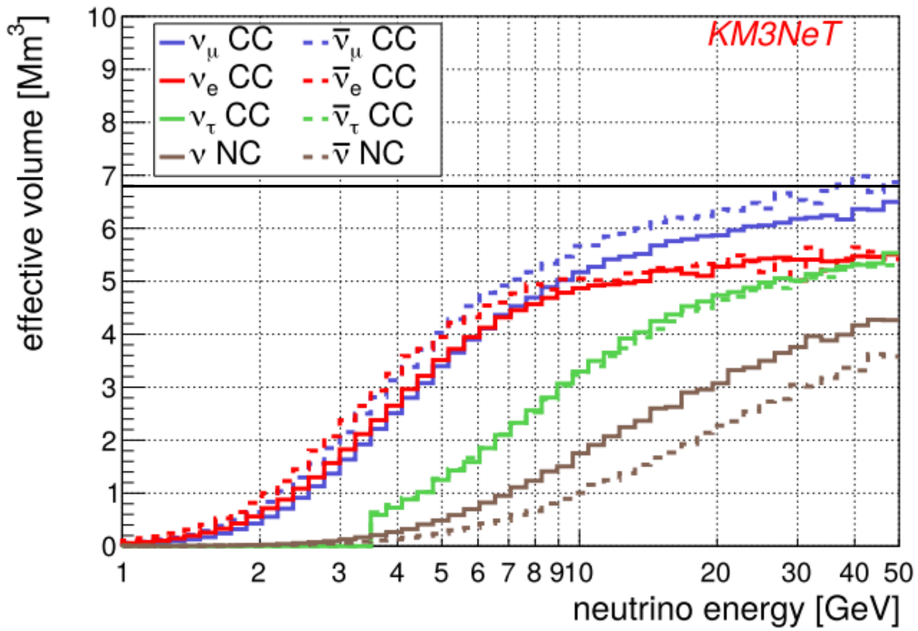

Figure 1: Effective detector volume as a function of true neutrino energy E_ν for different neutrino flavours and interaction types. Only events reconstructed and selected as upgoing have been used. The instrumented volume is $6.7\,\mathrm{Mm}^3$.

ORCA detector response

2.4 Event reconstruction and selection

- Why is the effective volume of reconstructed cos(zen) not following the true cos(zen)?

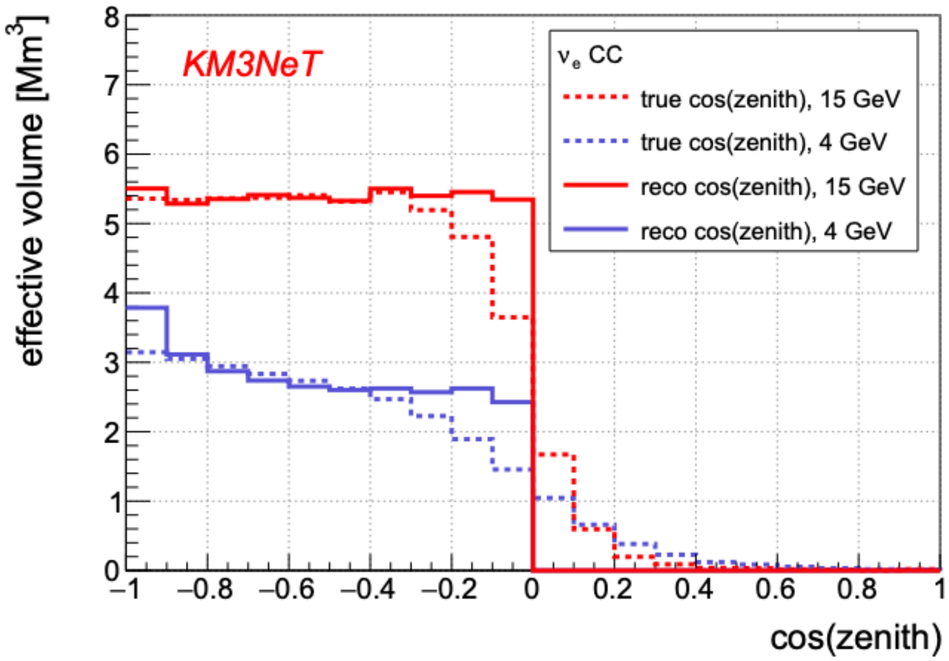

Figure 2: Effective detector volume as a function of reconstructed (solid) and true (dashed) cosine zenith angle $\cos\theta_z$ for ν_e CC events with $E_\nu \approx 4\,\mathrm{GeV}$ (blue) and $E_\nu \approx 15\,\mathrm{GeV}$ (red).

ORCA detector response

2.4 Event reconstruction and selection

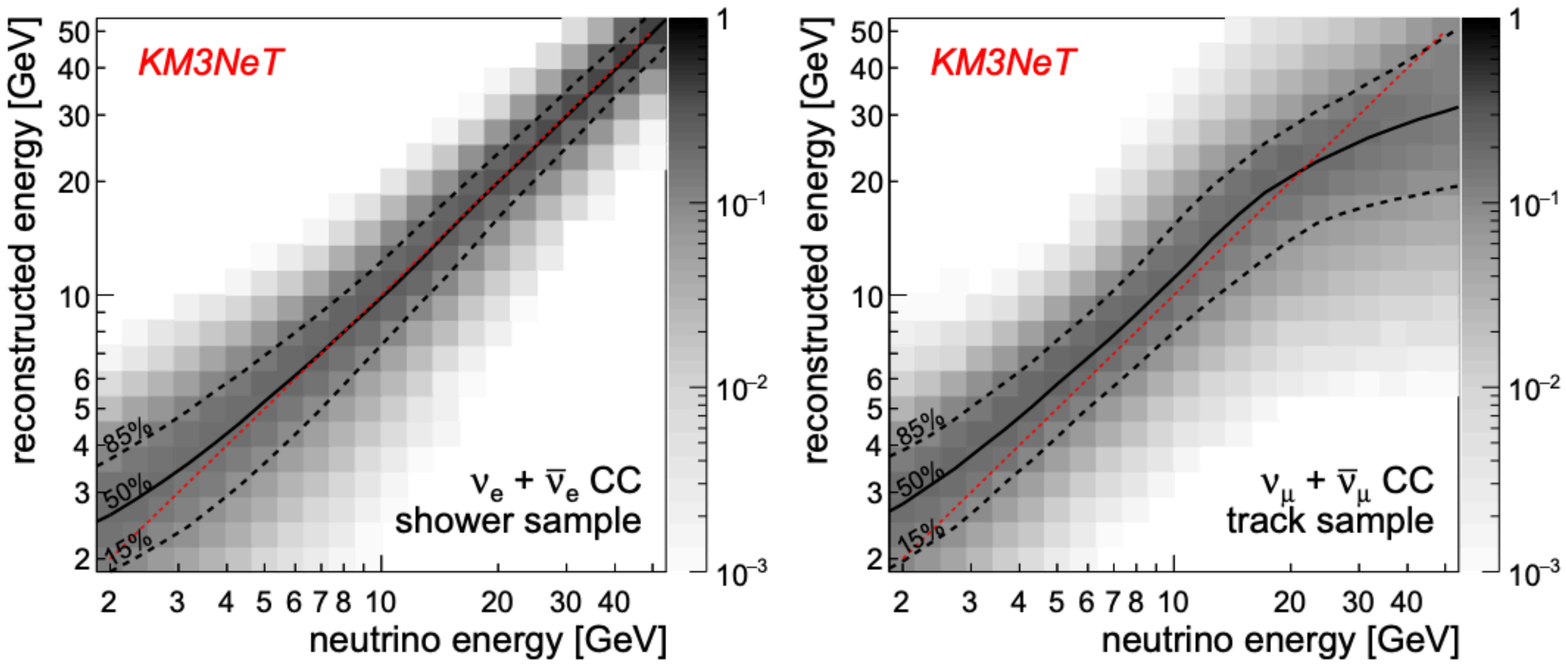

Figure 3: Probability distribution of the reconstructed energy as a function of true neutrino energy for upgoing ν_e CC and $\bar{\nu}_e$ CC events classified as shower-like (left)as well as ν_μ CC and $\bar{\nu}_\mu$ CC events classified as track-like (right). Solid and dashed black lines indicate 50%, 15% and 85% quantiles. For a definition of shower- and track-like events see Eq. 2. Correct reconstruction is indicated by the red diagonal line.

ORCA detector response

2.4 Event reconstruction and selection

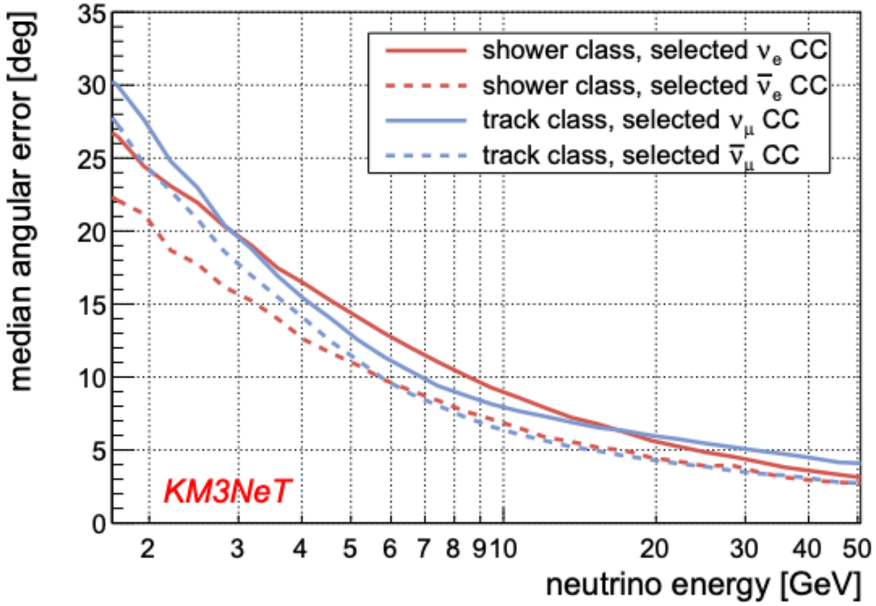

Figure 4: Median direction resolution as a function of true neutrino energy E_ν for upgoing ν_e CC and $\bar{\nu}_e$ CC events classified as shower-like as well as ν_μ CC and $\bar{\nu}_\mu$ CC events classified as track-like. For a definition of shower- and track-like events see Eq. 2.

ORCA detector response

2.5 Event classification

Three random decision forests (RDFs) score variables

1. *atmospheric_muon_score*
2. *noise_score*
3. *track_score*

ORCA detector response

2.5 Event classification

atmospheric_muon_score < 0.05

- 3% contamination
- 5% loss in neutrino efficiency

noise_score < 0.1

- Maintains neutrino efficiency

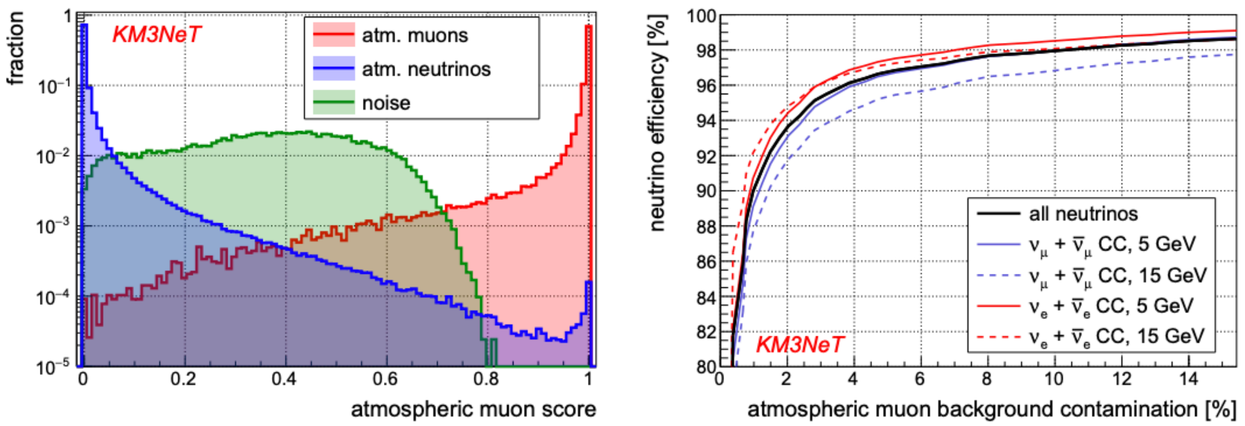

Figure 5: Left: Distribution of the atmospheric muon score variable for the RDF aimed to separate between neutrinos and atmospheric muons, for the main classes of events. Right: Fraction of remaining neutrinos weighted with an oscillated atmospheric flux versus atmospheric muon contamination in the final sample.

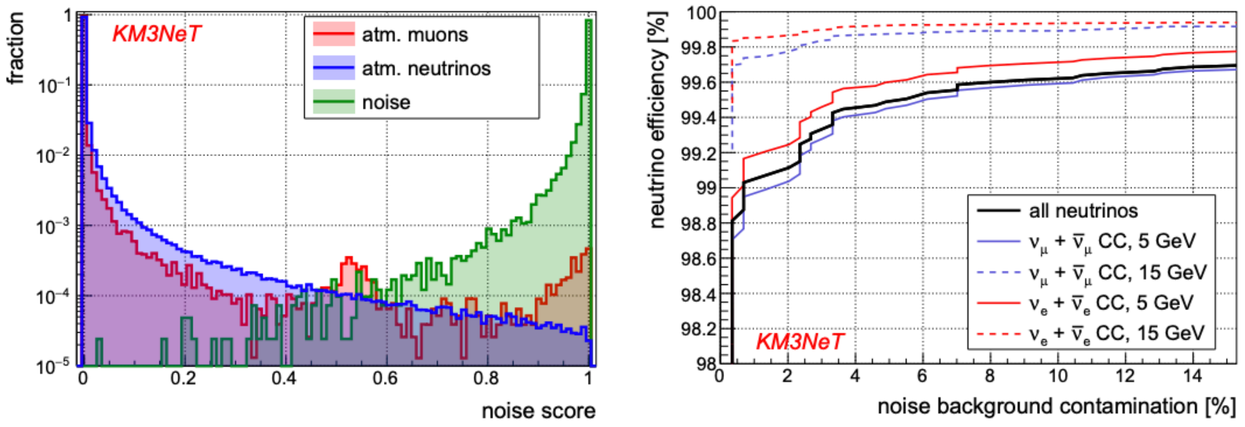

Figure 6: Left: Distribution of the noise score variable for the RDF aimed to separate between neutrinos and pure noise, for the main classes of events. Right: Fraction of remaining atmospheric neutrinos versus noise event contamination in the final sample.

ORCA detector response

2.5 Event classification

3 classes:

- **Shower**: *track_score* <= 0.3
- **Middle**: 0.3 < *track_score* <= 0.7
- **Track**: *track_score* > 0.7

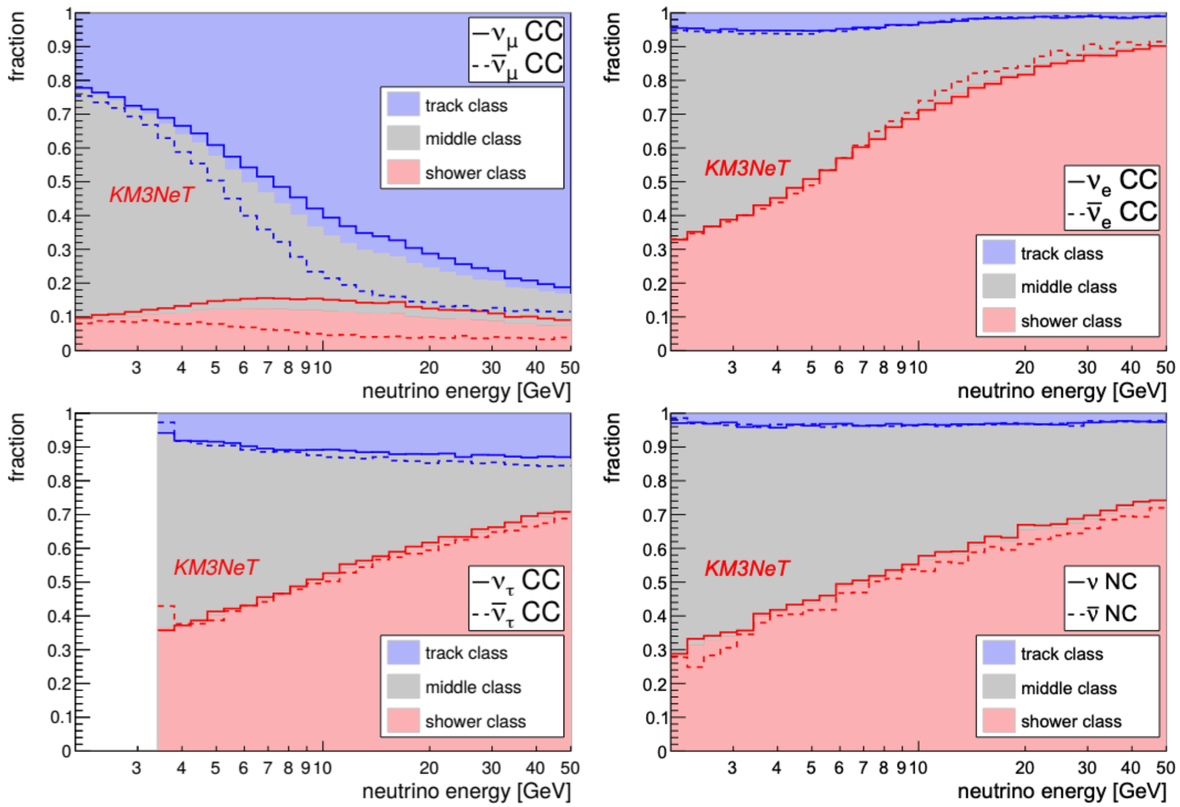

Figure 7: Fractions of preselected neutrino events of different types to be classified in the track class, the middle class, and the shower class, as a function of true neutrino energy. The definition of the classes is given in Eq. 2. Coloured areas correspond to the composition of the atmospheric neutrino flux. Solid and dashed lines show individual fractions for neutrinos and anti-neutrinos, respectively.

ORCA detector response

2.5 Event classification

$$\mathcal{S}(\Delta E) = 1 - \mathcal{C}(\Delta E) = 1 - \frac{\sum_i P^{\overleftrightarrow{\nu}_\mu}_{i,\text{score}}(\Delta E) \cdot P^{\overleftrightarrow{\nu}_e}_{i,\text{score}}(\Delta E)}{\sqrt{\sum_i \left(P^{\overleftrightarrow{\nu}_\mu}_{i,\text{score}}(\Delta E)\right)^2 \cdot \sum_i \left(P^{\overleftrightarrow{\nu}_e}_{i,\text{score}}(\Delta E)\right)^2}}.$$

Hit-based variables improves separation power

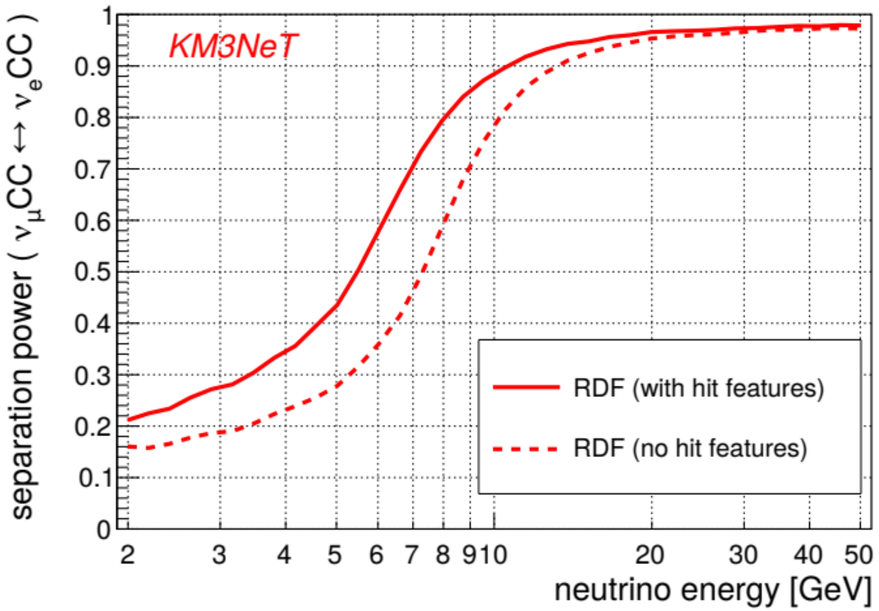

Figure 8: Comparison of the classifier performance as a function of true neutrino energy in terms of the separation power metric as defined in Eq. 3. Separation power for training with (solid) and without (dashed) hit-based features is shown.

Sensitivity calculation

3.1 method

$$\mathcal{L}_0^2 = \sum_{i \in [\mathrm{E^{rec}},\ \cos\theta_z^{\mathrm{rec}}]} \mathcal{L}_{0,i}^2$$
$$= \sum_{i \in [\mathrm{E^{rec}},\ \cos\theta_z^{\mathrm{rec}}]} -2.0 \cdot (n_i^{\mathrm{alt}} - n_i^{\mathrm{null}} - n_i^{\mathrm{alt}} \ln \frac{n_i^{\mathrm{alt}}}{n_i^{\mathrm{null}}}),$$

$$\mathcal{L}_{\mathrm{eff}}^2 = \mathcal{L}_0^2 + \sum_{i \in \mathrm{parameters}} \frac{(p_i^{\mathrm{exp}} - p_i^{\mathrm{obs}})^2}{\sigma_i^2}.$$

Uncertainties

- Spectral index
- Upgoing/horizontal
- ν_e/ν_μ
- $\nu_e/\bar{\nu}_e$
- $\nu_\mu/\bar{\nu}_\mu$
- NC scaling
- ν_τ CC scaling
- Energy scale
- Light yield hadronic showers
- Class scaling factor

Sensitivity calculation

3.2 NMO sensitivity

Table 1: Oscillation parameters values [6] used for the *null* hypothesis and the constraints applied during the $\mathcal{L}^2_{eff}$ minimisation.

Parameter		Null Hypothesis Values	Constraints
Δm^2_{21}		$7.39 \cdot 10^{-5}$ eV^2	fixed
θ_{12}		$33.82°$	fixed
θ_{13}	NO IO	$8.60°$ $8.64°$	$\pm 0.13°$
Δm^2_{31}	NO IO	$2.528 \cdot 10^{-3}$ eV^2 $2.436 \cdot 10^{-3}$ eV^2	free
θ_{23}	NO IO	$48.6°$, $[40°–50°]$ $48.8°$, $[40°–50°]$	free
δ_{CP}	NO IO	$221.0°$, $0°$, $180.0°$ $282.0°$, $0°$, $180.0°$	free

Value outside constraints?

Sensitivity calculation

3.2 NMO sensitivity

How do you read the right plots?

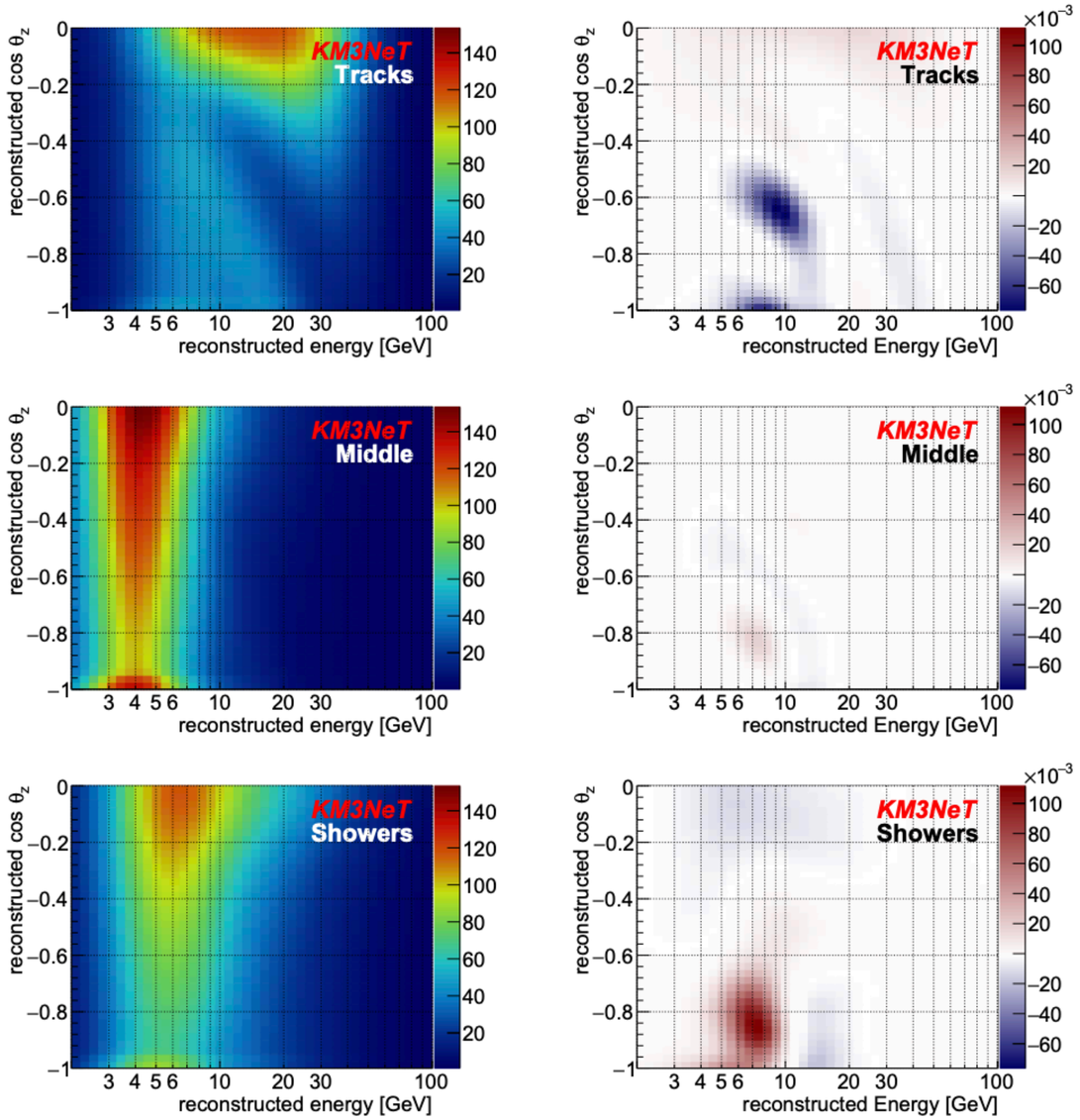

Figure 9: Expected event distributions for NO after 3 years of data taking (left) for events classified as track (top) middle (middle) and shower (bottom) and the $\mathcal{L}^2_{0,i}$ (right) between these distributions and the ones obtained minimising $\mathcal{L}^2_{\text{eff}}$ with the IO hypothesis.

Sensitivity calculation

3.3

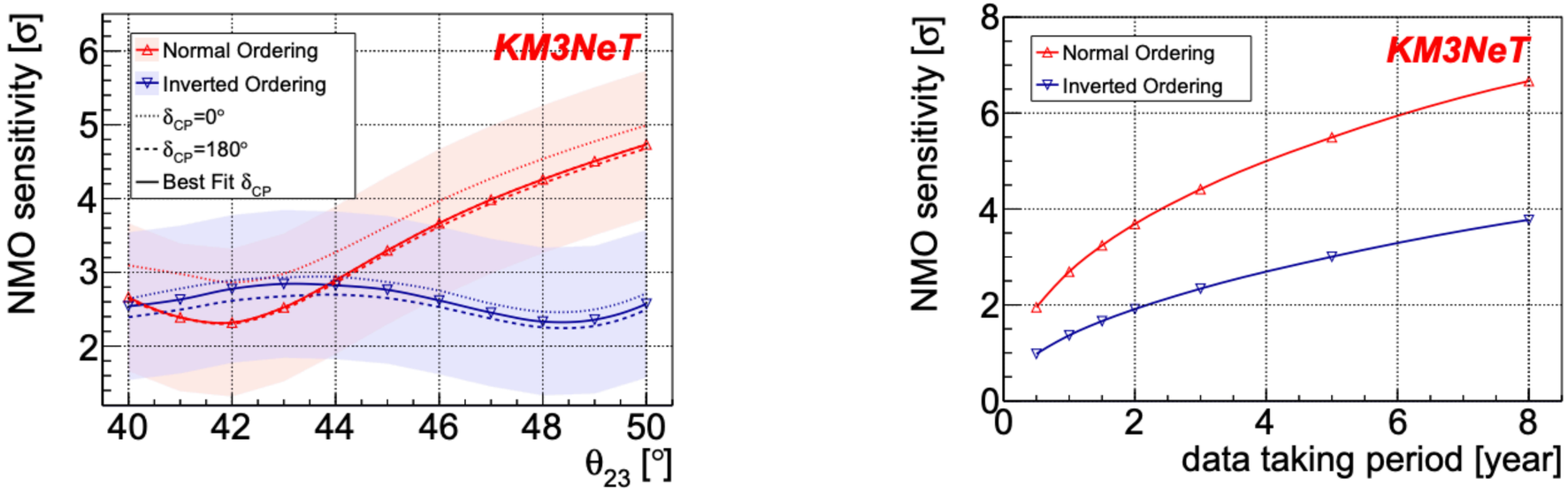

(a) (b)

Figure 10: (a) Sensitivity to NMO after three years of data taking, as a function of the true θ_{23} value, for both normal (red upward pointing triangles) and inverted ordering (blue downward pointing triangles) under three assumptions for the δ_{CP} value: the world best fit point for NO, IO reported in Table 1 (plain line), 0° (dotted line) or 180° (dashed line). The coloured shaded areas represent the sensitivity that 68% of the experiment realisation would yield, according to the Asimov approach [42]. (b) Sensitivity to NMO as a function of data taking time for both normal (red upward pointing triangles) and inverted ordering (blue downward pointing triangles) and assuming the oscillation parameters reported in Table 1.

Sensitivity calculation

3.3

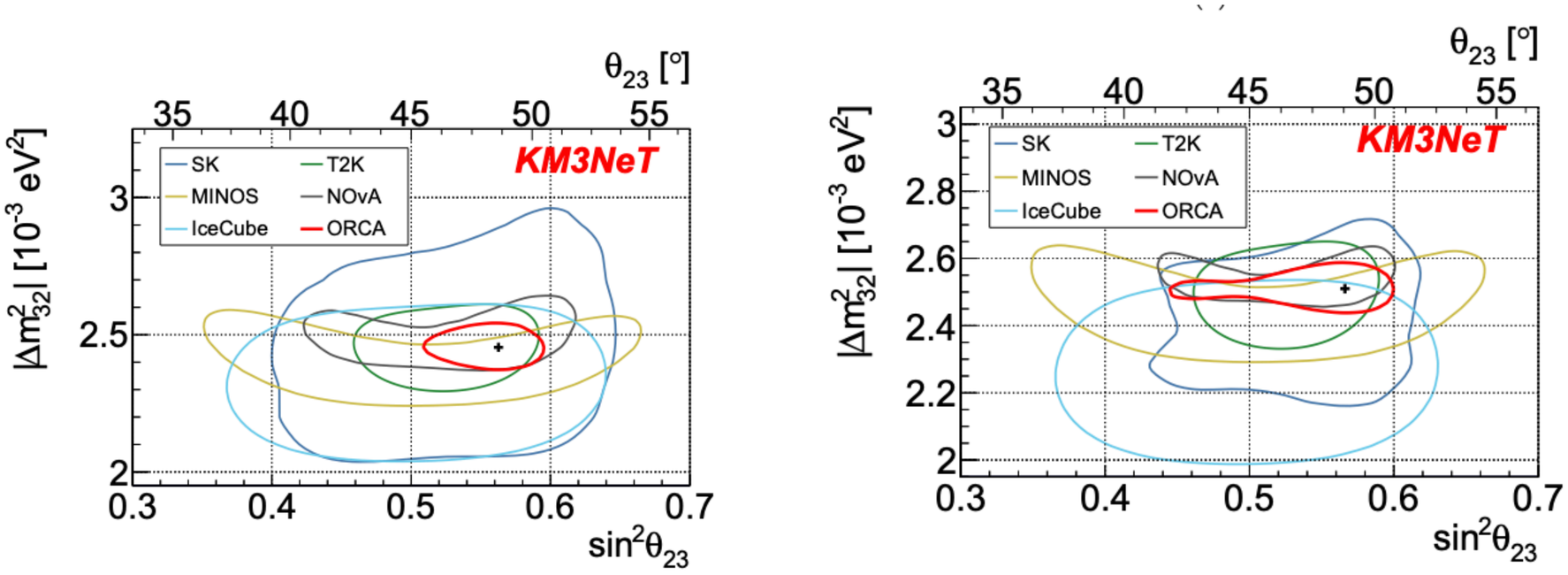

(a) (b)

Figure 11: Expected measurement precision of Δm^2_{32} and θ_{23} for both NO (a) and IO (b) after 3 years of data taking at 90% CL (red) overlaid with other experiments results [14, 13, 10, 12, 11] and the oscillation parameters reported in Table 1 (black cross).

Sensitivity calculation

3.3

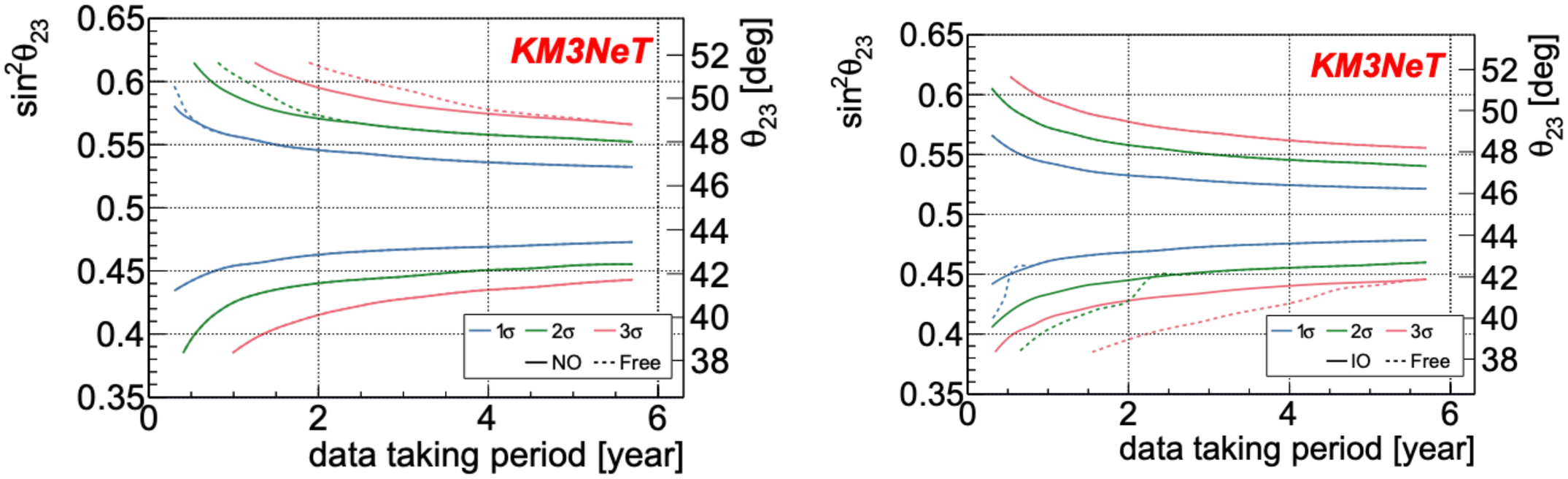

(a) (b)

Figure 12: Expected sensitivity to determine θ_{23} octant at 1 (blue), 2 (green) or 3 (red) σ as a function of data taking time for both NO (a) and IO (b) assuming the true NMO is known (solid line) or unknown (dashed line).

Sensitivity calculation

3.4 Tau

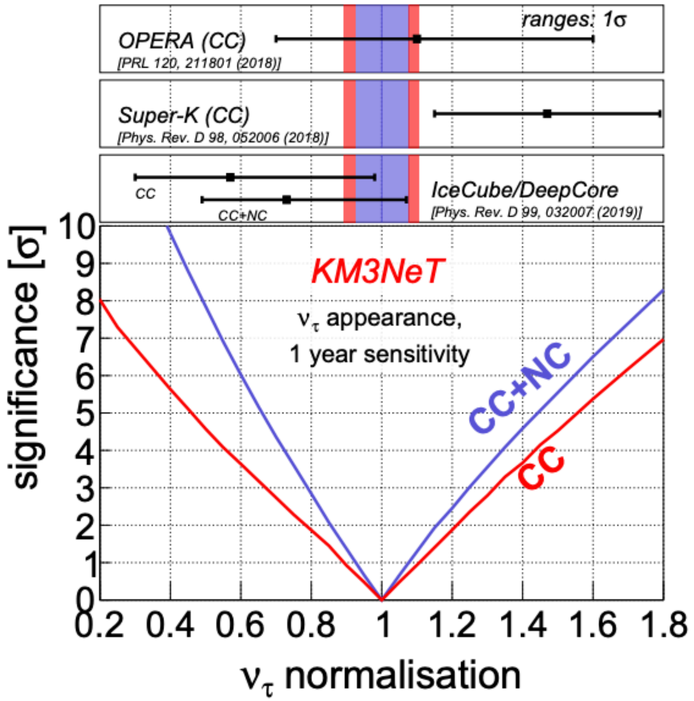

(a)

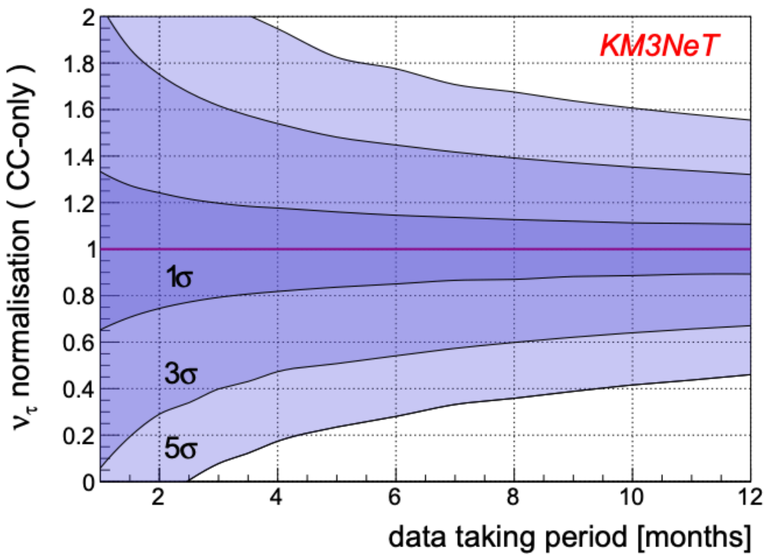

(b)

Figure 13: Sensitivity to $\overset{(-)}{\nu}_\tau$ appearance for CC and CC+NC normalisation scaling after one year of operation (a). Experimental results from other experiments [47, 48, 49] at 1σ level are shown for comparison. In (b), $\overset{(-)}{\nu}_\tau$ appearance sensitivity for CC scaling is presented as a function of data-taking period.

Conclusions

- What is the improvement with respect to last time?